A Bimodal Pattern of $InsP_3$-Evoked Elementary Ca^{2+} Signals in Pancreatic Acinar Cells

K. E. Fogarty,* J. F. Kidd,† R. A. Tuft,* and P. Thorn†

*Biomedical Imaging Group, Department of Physiology, University of Massachusetts Medical School, Worcester, Massachusetts 01650 USA, and †Department of Pharmacology, University of Cambridge, Cambridge CB2 1QJ, United Kingdom

ABSTRACT $InsP_3$-evoked elementary Ca^{2+} release events have been postulated to play a role in providing the building blocks of larger Ca^{2+} signals. In pancreatic acinar cells, low concentrations of acetylcholine or the injection of low concentrations of $InsP_3$ elicit a train of spatially localized Ca^{2+} spikes. In this study we have quantified these responses and compared the Ca^{2+} signals to the elementary events shown in *Xenopus* oocytes. The results demonstrate, at the same concentrations of $InsP_3$, Ca^{2+} signals consisting of one population of small transient Ca^{2+} release events and a second distinct population of larger Ca^{2+} spikes. The signal mass amplitudes of both types of events are within the range of amplitudes for the elementary events in *Xenopus* oocytes. However, the bimodal Ca^{2+} distribution of Ca^{2+} responses we observe is not consistent with the continuum of event sizes seen in *Xenopus*. We conclude that the two types of $InsP_3$-dependent events in acinar cells are both elementary Ca^{2+} signals, which are independent of one another. Our data indicate a complexity to the organization of the Ca^{2+} release apparatus in acinar cells, which might result from the presence of multiple $InsP_3$ receptor isoforms, and is likely to be important in the physiology of these cells.

INTRODUCTION

Spatial and temporal shaping of intracellular Ca^{2+} signals are known to be important factors in conferring specificity in the regulation of Ca^{2+}-dependent targets (Nelson et al., 1995; De Koninck and Schulman, 1998; Dolmetsch et al., 1998; Deisseroth et al., 1998). However, we are only just beginning to understand the mechanisms that establish these complex Ca^{2+} signals (Berridge, 1997). In particular, although Ca^{2+} release from intracellular Ca^{2+} stores is known to be important in Ca^{2+} signaling, the fundamental mechanisms of Ca^{2+} release are unclear. Study of the regulation of $InsP_3$ receptors has given insights in to characteristics of $InsP_3$-mediated Ca^{2+} release that may be important in the control of the Ca^{2+} signal (Taylor, 1998). In vivo, measurements suggest that $InsP_3$ receptors are clustered in patches on the intracellular Ca^{2+} store membrane (Mak and Foskett, 1997). Functionally, at low levels of stimulation, this clustering gives rise to spatially and temporally discrete "Ca^{2+} puffs" (Mak and Foskett, 1997; Yao et al., 1995). Analysis of individual puffs has shown a variation in Ca^{2+} signal mass or Ca^{2+} amplitude with distributions consistent with a single population of events (Sun et al., 1998; Thomas et al., 1998). These "elementary" events have been postulated to have a local role on effector systems and also to provide the building blocks of Ca^{2+} signaling. In this way, at higher stimulus levels, the spatial and temporal summation of the elementary events is proposed to be the mechanism that underlies the complex Ca^{2+} patterns seen in cells (Berridge, 1997; Bootman et al., 1997b; Callamaras et al., 1998).

In pancreatic acinar cells, agonists elicit spatially discrete $InsP_3$-dependent Ca^{2+} spikes within a specialized region of the cell (Thorn et al., 1993; Kasai et al., 1993). These local Ca^{2+} spikes have been shown to be important in activating mechanisms of fluid and enzyme secretion (Ito et al., 1997). The local Ca^{2+} signal is thought to be structurally complex, with regional "hot spots" of Ca^{2+} release (Thorn et al., 1996) and local gradients of Ca^{2+} (Ito et al., 1997). Furthermore, we have recently shown that local $InsP_3$-evoked spikes result from patterns of regional Ca^{2+} release coordinated by a process of Ca^{2+}-induced Ca^{2+} release (CICR) (Kidd et al., 1999). This mechanism of CICR has been suggested to be central to the agonist-evoked responses (Ito et al., 1999).

To understand these complexities in the formation of the local Ca^{2+} signal we have now used high spatial and temporal resolution imaging techniques. Our experiments quantify the Ca^{2+} signals in terms of the amount (signal mass) of Ca^{2+} released (Sun et al., 1998) and enable a direct comparison with the "puff" and "blip" events in *Xenopus* oocytes (Sun et al., 1998) that are thought to be the elementary building blocks of Ca^{2+} release. Our results quantify, over a range of fixed concentrations of $InsP_3$, two apparently independent elementary Ca^{2+} release events. The larger of these behaves as a unitary Ca^{2+} signal that, although it is similar in size, is kinetically different from previously reported "puffs." We conclude that our results contrast with previous reports of a continuum of elementary Ca^{2+} events and suggest more complex mechanisms of regional Ca^{2+} release in the pancreatic acinar cell.

Received for publication 29 November 1999 and in final form 7 February 2000.

Address reprint requests to Peter Thorn, Dept. of Pharmacology, University of Cambridge, Tennis Court Road, Cambridge CB2 1QJ, UK. Tel.: 01223 334017; Fax: 01223 334040; E-mail: pt207@cus.cam.ac.uk.

0006-3495/00/05/2298/09 $2.00

MATERIALS AND METHODS

Cell preparation

Male outbred albino mice (25 g) were killed by cervical dislocation and the pancreas dissected out. Acutely isolated mouse pancreatic acinar cells were prepared by collagenase (Worthington, CLSPA, Lorne Labs., Lakewood, N.J.) digestion at 33°C for 7 min as previously described (Thorn and Petersen, 1992). Cells were plated on to poly-L-ornithine (Sigma, Poole, UK) coated coverslips. We recorded from single cells and cells within a small clump (2–4 cells). Cell polarity was obvious from the location of secretory granules and cell orientation within a cluster.

Patch clamp

Standard whole-cell patch clamp techniques (Hamill et al., 1981) were used and all experiments were carried out at room temperature (~21°C). Pipettes had a resistance of 3–6 MΩ (pipette puller, Brown and Flaming, Sutter Instrument Co., Novato, CA). After breaking through to the whole-cell configuration pipettes had a measured, but uncompensated, series resistance of 10–20 MΩ. The pipette solution contained (in mM): 140 KCl, 1 $MgCl_2$, 2 Na_2ATP, 0.2 EGTA, (0.05 Calcium Green, Molecular Probes, Eugene, OR), 10 HEPES-KOH, pH 7.2. The extracellular solution contained (in mM): 135 NaCl, 5 KCl, 1 $MgCl_2$, 1 $CaCl_2$, 10 glucose, 10 NaOH-HEPES, pH 7.4. Cells were held at a membrane potential of −30 mV and currents were sampled by an A/D converter at 1 KHz. In all experiments Ins(2,4,5)P_3 (a gift from Professor R. Irvine) was added to the pipette solution (6, 8, 10, 12 μM) to establish trains of Ca^{2+} spikes which, in the whole-cell recordings, led to the activation of Ca^{2+}-dependent current spikes. The Ca^{2+} spikes have previously been shown to originate from a mechanism of $InsP_3$-dependent Ca^{2+} release in the secretory pole (Thorn et al., 1993), to remain localized to this region of the cell, and to be independent of ryanodine receptor activity (Thorn et al., 1994). We have shown previously that under our conditions, the whole-cell current is predominantly carried by a $Cl_{(Ca)}$ channel (Kidd et al., 1999).

Fluorescence imaging

The $InsP_3$-evoked trains of Ca^{2+} spikes were established over a period of up to 40 min (the lifetime of the whole-cell patch recording). These spikes were continuously observed in the whole-cell $Cl_{(Ca)}$ currents. However, due to limitations of computer storage capacity, only short sequences of fluorescent images, up to 20 s long, could be captured. After data storage another image sequence could be captured, and this process was repeated up to five times in one cell.

The Ca^{2+} imaging experiments were performed by inclusion of 40–50 μM Calcium Green (Molecular Probes, Eugene, OR) in the pipette solution. Cells were illuminated with a visible laser (Coherent Innova 70, Santa Clara, CA) at 488 nm and imaged through a Nikon 40× UV, 1.3NA, oil immersion objective through a 510-nm-long pass filter. Full frame images (128 × 128 pixels) were captured on a cooled CCD camera (70% quantum efficiency, 5 electrons readout noise at 500 frames per second; MIT, Lincoln Laboratory) with a pixel size of 200 nm at the specimen. All images were acquired at 20 frames per second (50 ms between images) and with either 5- or 10-ms exposures controlled by a Uniblitz shutter (Vincent Associates, Rochester, NY). After recording to the computer, the data were analyzed with custom software following appropriate bleach correction and smoothing. Images were displayed as $\Delta F/F_o$ images ($100 \times (F - F_o)/F_o$), where F is the recorded fluorescence and F_o was obtained from the mean of 20 sequential frames where no activity was apparent. The principle advantage of this imaging technique is the fast rate of acquisition of full-frame images (Rizzuto et al., 1998).

Ca^{2+} signal mass units

Ratiometric measurement is proportional to the concentration of Ca^{2+}; in contrast, the signal mass unit is proportional to the amount of released Ca^{2+}. This means that as the Ca^{2+} signal diffuses away from the release site the ratiometric measure of concentration will go down, but the signal mass unit will stay high. Calculations of calcium signal mass, i.e., the amount of Ca^{2+} released in a single event, were done directly from the two-dimensional, wide-field fluorescence images of Calcium Green. For the smaller Ca^{2+} release events, signal mass was measured as the change in total fluorescence within a square region, 5 × 5 μm (25 × 25 pixels), centered over the events as identified manually from the spatial and temporal peak in the $\Delta F/F_0$ images. Custom software was then used to process the images and extract signal mass information for each release event. The beginning of the release event was identified as the first image where the increase in total fluorescence from the preceding frame (50 ms) exceeded 2 SDs of the RMS noise of the difference between frames. RMS noise was calculated directly from the photon statistics of the image; the high-speed CCD camera was previously calibrated as having a linear response to light with a sensitivity of 5 photons per digital count and 5 photon equivalent RMS readout noise at each pixel. The end of the release event was taken as the last consecutive image having a significant increase (same criterion) in total fluorescence from the preceding frame. The peak signal mass was calculated as the difference in the total fluorescence between the end image and that preceding the beginning of the event.

As a consequence of the wide-field imaging arrangement used, photons emitted from Calcium Green molecules outside of the plane of focus are still collected and imaged onto the camera. The 5 × 5 μm square size of the region used was chosen to capture fluorescence due to Ca^{2+} diffusing away from the site of release and to allow for the apparent increased spatial spread of release events that were out of focus. For the larger events, changes in total fluorescence were measured from the whole cell. For these events the identification of the beginning and ending of the change in signal mass was done manually.

Calibration of signal mass into moles of Ca^{2+} was made assuming a Calcium Green concentration of 50 μM, K_d = 190 nM (Molecular Probes), and a resting [Ca^{2+}] of 50 nM. Assuming a spherical cell with an average diameter of 15 μm, the imaged "volume" within the 5 × 5 μm region used for the smaller events was calculated, as was the fraction of Calcium Green bound to Ca^{2+}. The resting fluorescence resulting from the bound Calcium Green within this volume was measured, and an average signal of 0.4083 photons per Ca^{2+} ion bound to Calcium Green was calculated. The contribution to the fluorescence signal from the Ca^{2+}-free indicator was calculated to be <2%, and ignored. From this relationship, the amount of Ca^{2+} required to double the fluorescence in 1 fl, which we define as one signal mass unit (smu) in accordance with Sun et al. (1998), is $\sim 10^{-20}$ moles. Using this calibration, our average detection threshold for small events was a change of ~0.8 smu in 50 ms, and the smallest threshold was ~0.4 smu in 50 ms.

There are problems with the use of signal mass units. The released Ca^{2+} is partitioned not only into the fluorescent dye, but also into the other buffers. These include the endogenous buffer as well as EGTA and ATP in our pipette solution. The signal reported by the dye will therefore be dependent on the dye and other exogenous buffer concentrations as well as the endogenous buffer concentration. Our experiments minimize this problem in two ways. First, the use of patch clamp delivery of dye gives a lot less cell to cell variability than other techniques. Second, all the cells used in our study showed both smaller events and spikes, allowing a direct comparison of signal mass unit size.

Detection of the events

Our criteria for the detection of the smaller events were a Ca^{2+} signal that was small (peak < 10% $\Delta F/F_0$), spatially discrete, and transient. These were initially identified by eye and therefore the data most probably

represent the largest events in this population, with smaller signals being lost in the noise. Having identified the spatial location and time frame of each event we then used a custom-made program to identify the time of the first significant increase in Ca^{2+} signal mass units (>2 SDs of the RMS noise calculated for each individual experiment). This was then used to align the time courses of the events and produce the averages shown in Figs. 4 and 6. The spikes were identified on the criteria that the average Ca^{2+} signal, measured across the entire cell, exceeded a $\Delta F/F_o$ of 5%. This time point was also used to calculate the time to peak of the spikes. The peak Ca^{2+} signal mass unit was measured as the peak signal mass minus the signal mass taken before the time point identified by the 5% change. In Fig. 7 the individual Ca^{2+} signal mass time courses were aligned to the peak of the Ca^{2+} signal mass.

The graph of Fig. 5 was produced by including all Ca^{2+} signals observed, all of which were transient and all were spatially discrete. In none of the records did we find evidence for sustained Ca^{2+} signals. Our probable bias in identifying the larger of the small events would tend to overestimate the mean size of these events. Furthermore, we would expect EGTA to have a greater impact on the slower Ca^{2+} spikes, leading to an underestimate of their amplitude. Using computer reaction-diffusion simulations, as previously described (Zou et al., 1999), of both the small Ca^{2+} signals and the larger, longer-lived spikes, we investigated the possible effect of EGTA, a slow Ca^{2+} buffer, on the measurement of the Ca^{2+} signal masses using Calcium Green. In these simulations, the effect of the addition of 200 μM EGTA on the small, faster events was to underestimate the signal mass by <7%. The effect on the spikes was larger, leading to an underestimate of ~50%. These measurement errors would make the ~100× difference in mean size between the small events and the spikes we observe, an underestimate.

RESULTS

Trains of Ca^{2+} spikes, induced by the injection of 8–12 μM Ins(2,4,5)P_3 (Thorn et al., 1993, 1996; Wakui and Petersen, 1990), were studied in isolated mouse pancreatic acinar cells. This $InsP_3$-evoked signal has previously been shown to be very reproducible and trains of spikes can be recorded for up to 40 min, enabling us to repeatedly record imaging segments from the same cell (Kidd et al., 1999). Cells were whole-cell patch clamped and the Ca^{2+} signal monitored with Calcium Green (40–50 μM). The secretory pole of single acinar cells was identified by the localization of zymogen granules. Secretory pole Ca^{2+} spikes (Fig. 1, region 1, frequency of 0.083 Hz, $n = 39$ from 14 cells) were observed, as previously described (Kasai et al., 1993; Thorn et al., 1993). With high-resolution imaging techniques we observe that the majority of secretory pole spikes do not encompass the whole of the secretory pole region. This is shown in Fig. 1 where the spike (Fig. 1, *image b*) extends only over ~5 μm diameter (full-width at half-maximum (FWHM) signal area = 30.76 ± 2.44 μm^2, mean ± SEM, $n = 28$) within the secretory pole. In addition to the spikes, our sensitive imaging techniques now also detected smaller Ca^{2+} events (peak Ca^{2+} <10% $\Delta F/F_o$, Fig. 1, *image c*) that have not previously been observed in acinar cells. In the cell shown in Fig. 1 the spike and the smaller event arise from separate sites within the secretory pole and show very little cross-talk in the regional Ca^{2+} signals. The simultaneously acquired whole-cell current is also shown (Fig. 1, *image b*)

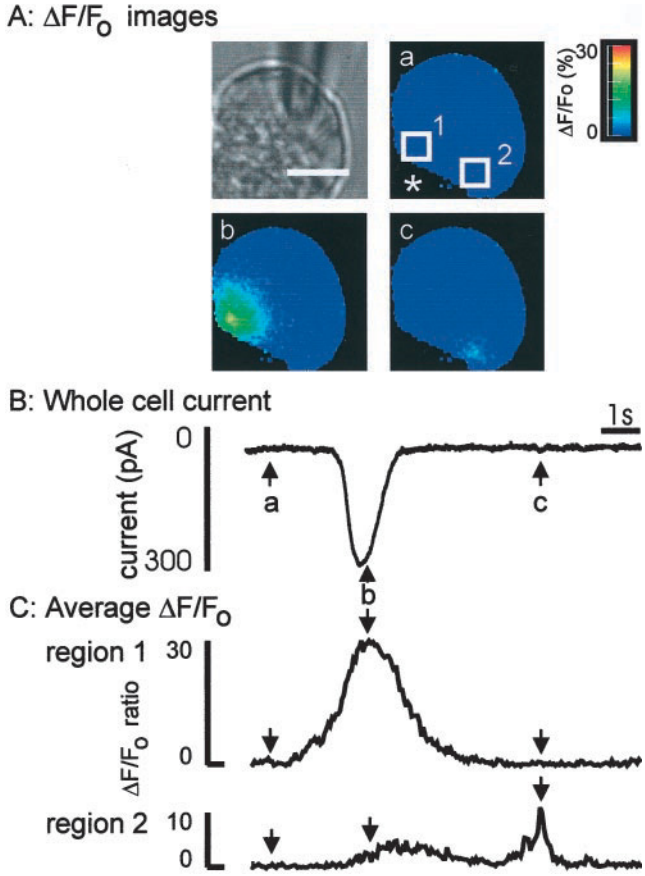

FIGURE 1 The Ca^{2+} signal and whole-cell current in response to Ins(2,4,5)P_3. Typically, $InsP_3$ evoked a train of short-lasting $Cl_{(Ca)}$ spikes, and the Ca^{2+} recordings shown represent short sequences (~20 s) of captured images from the total response. A single larger Ca^{2+} spike is shown followed by a smaller Ca^{2+} event. Both Ca^{2+} release events occur locally within the secretory pole region, identified by the location of the secretory granules as seen in transmitted light (black and white) image of *A*, which also shows the patch pipette. The scale bar indicates 10 μm. *A* also shows three pseudocolor, fluorescence ratio images taken at time points (*a*) resting Ca^{2+}, (*b*) the peak of the larger spike, and (*c*) the peak of the smaller event. The asterisk indicates the secretory pole orientation of the cell, in this image and in all other figures. The boxes outline the 5 × 5-μm-square regions used to calculate the average Ca^{2+} signal shown in *C*. *B* shows the simultaneously recorded whole-cell current obtained under voltage clamp at a membrane potential of −30 mV. *C* shows the mean $\Delta F/F_o$ (×100) record within regions 1 and 2 shown in *A*(*a*). In this figure and in Fig. 2 we have selected examples of the small events that can clearly be seen in single pseudocolor images. As a consequence, these events are at the upper end of the smaller-event amplitude distribution.

and demonstrates a current spike approximately synchronous with the Ca^{2+} spike, but little response during the smaller Ca^{2+} event. Some Ca^{2+} spikes we recorded were larger in peak amplitude and spread (10/39 secretory pole spikes) but still occurred within the secretory pole. An example of a large spike response is shown in Fig. 2 (*image d*). This cell also shows evidence for a smaller Ca^{2+} event (Fig. 2, *image a*) preceding the large Ca^{2+} spike. In this

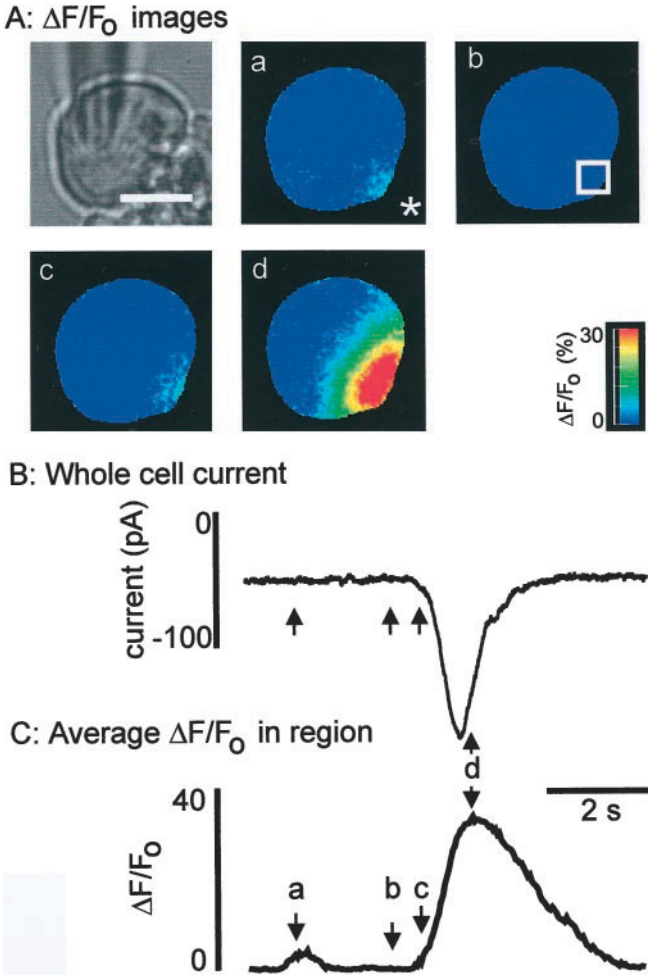

FIGURE 2 An example of the Ca^{2+} signal in response to $Ins(2,4,5)P_3$ where the larger Ca^{2+} spike is preceded by a smaller Ca^{2+} signal arising from the same position within the secretory pole. *A* shows the transmitted light (black and white) image and the pseudocolor fluorescence ratio images taken at three time points: (*a*) the peak of the smaller event, (*b*) resting Ca^{2+}, (*c*) during the rising phase of the larger spike, and (*d*) the peak of the larger spike. The box in *b* outlines the 5 × 5-μm-square region used to calculate the average Ca^{2+} signal shown in *C*. The scale bar is 10 μm. *B* shows the simultaneously recorded whole-cell current obtained under voltage clamp at a membrane potential of −30 mV. *C* shows the mean $\Delta F/F_o$ (×100) record within the region shown in *A*(*b*). The large Ca^{2+} signal is nearly synchronous with the large current spike, but there is no evidence of a current associated with the smaller Ca^{2+} event.

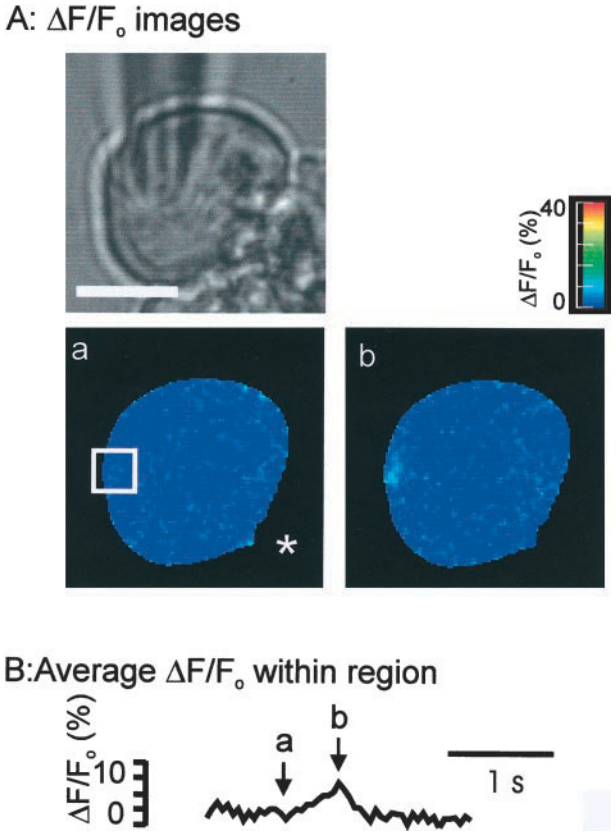

FIGURE 3 An example of a single small Ca^{2+} release event in the basal pole. *A* shows the transmitted (black and white) image of the cell and the patch pipette. The pseudocolor fluorescence ratio image in *a* was taken immediately preceding the event; *b* was taken at the peak of the small event. *B* is the average Ca^{2+} signal within the 5 × 5-μm-square region indicated by the box in *a*.

case, the two responses apparently arise from the same region of the cell.

Although larger spikes were never observed in the basal pole, we did find evidence of smaller Ca^{2+} release events occurring in this region of the cell (Fig. 3). It therefore appears as if the smaller events and the larger spikes may, but do not necessarily, arise from the same regions of the cell.

The small Ca^{2+} release events occurred randomly in time throughout the records and were not correlated with the rising or falling phases of the larger secretory pole Ca^{2+} spike. Across the secretory pole the small events had a frequency of 0.106 Hz, compared to a slightly higher frequency of 0.142 Hz for events in the basal pole. In some cells evidence for up to eight spatially distinct release sites was obtained, with some sites giving rise to repeated events. The average ratio images of basal pole ($n = 54$) and secretory pole ($n = 55$) small Ca^{2+} release events, aligned to the rising phase of the Ca^{2+} signal, are shown in Fig. 4. The Ca^{2+} signal rose to a peak in 50–100 ms and then decayed over 100–200 ms to baseline. Although apparently different in the images shown, the mean rates of decay of the Ca^{2+} signal were not significantly different in both regions of the cell. The mean area of these signals was 9.48 μm^2 (FWHM). Assuming an average cell diameter of 15 μm, these small events would encompass ~1.2% of cell volume compared to ~7% of cell volume for the larger secretory pole spikes.

In control experiments, with a slightly lower concentration of 6 μM $InsP_3$ ($n = 3$ cells), neither Ca^{2+} spikes nor small Ca^{2+} release events were ever observed. At the higher concentrations of $InsP_3$ used, 8, 10, and 12 μM, there was

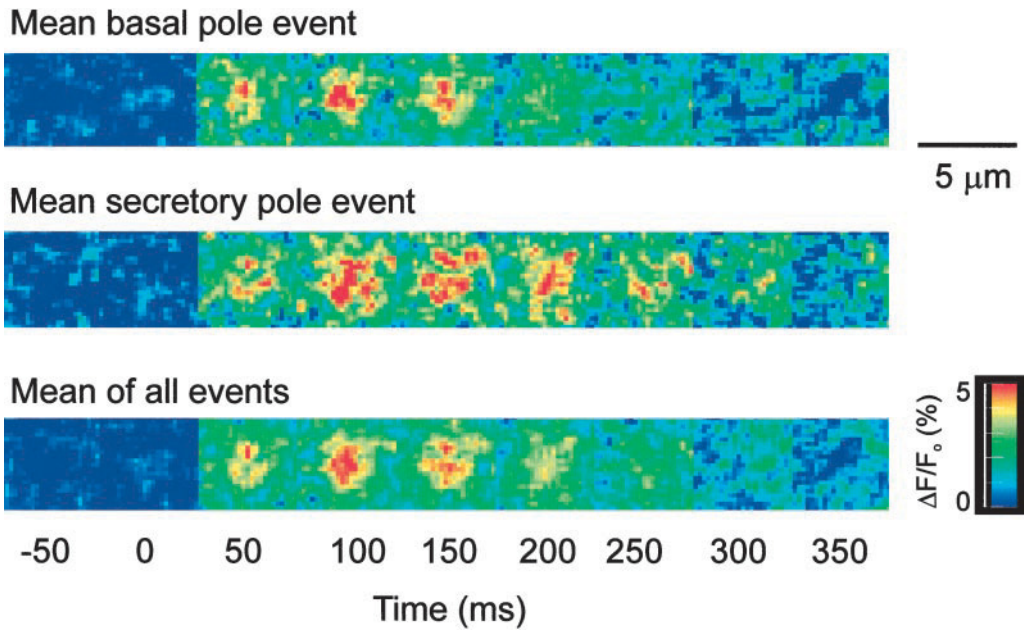

FIGURE 4 A pseudocolor fluorescence ratio representation of the averages of all the smaller Ca^{2+} events recorded in the basal and secretory poles. The spatial position and time course were recorded for each event ($n = 96$) identified in 560 s of images obtained from 14 cells. To make the average images, all events were aligned in time at the point where the signal mass measurement first exceeded the noise, and in space at the pixel having the maximum $\Delta F/F_o$. No significant difference was found in time course or amplitude between the events in the two poles, and the mean of all events is therefore also shown.

no significant difference in frequency or amplitude for either the Ca^{2+} spikes or the small Ca^{2+} events. This indicates that both the small events and the larger spikes have the same threshold for $InsP_3$-dependent activation.

We conclude that the cellular response to $InsP_3$ consists of a dual pattern of localized Ca^{2+} signals. Both signals appear comparable in amplitude and kinetics to the range of Ca^{2+} elementary events seen in *Xenopus* oocytes and other cells (Sun et al., 1998; Thomas et al., 1998).

We therefore set out to characterize the two different types of responses in order to determine whether they represent two entirely different modes of Ca^{2+} release or are at extremes of a single population of events. Analysis of Ca^{2+} "elementary event" signal mass in *Xenopus* oocytes and Ca^{2+} amplitudes in HeLa cells has indicated that the discrete Ca^{2+} release events do represent a single population (Sun et al., 1998; Thomas et al., 1998). We therefore set out to measure the Ca^{2+} signal mass amplitudes of Ca^{2+} release to determine whether this was the case in acinar cells. We used a definition of one signal mass unit as equal to a doubling of fluorescence in 1 fl volume, which under our conditions is equal to 10^{-20} moles of Ca^{2+}. This is the same unit as that used by Sun et al. (1998) in their analysis of elementary events in *Xenopus* oocytes. All cells showed secretory pole spikes and most also showed smaller events in the basal and secretory pole. Importantly, no other types of Ca^{2+} release were observed; that is, our analysis encompassed all the $InsP_3$-evoked Ca^{2+} responses. The histogram of Ca^{2+} signal mass units showed no overlap in the sizes of the small Ca^{2+} events with the sizes of the smallest spikes, and there was a clear separation in the modal values of the two distributions. The histograms of the smaller events in the basal pole and secretory pole (Fig. 5 *A*) were very similar in signal mass distribution and apparently arise from a similar population of events (Ca^{2+} signal mass populations not significantly different, $p = 0.5696$, Mann-Whitney U test, shown combined in Fig. 5 *A*, *bottom*). In contrast, the histogram of the larger spikes (Fig. 5 *B*) had a second mode, or peak, ~100 times larger than the mode of the smaller events. Overall, these data show a >3000-fold difference between the smallest and largest event (Fig. 5 *B*). Although Gaussian and exponential distributions could be fitted to our data we were reluctant to do so, as this implies knowledge of the underlying process. The data clearly cannot be fitted by a single Gaussian or a single exponential, indicating that multiple processes must be present. For example, while a single exponential could be fitted to the smaller events, this distribution would not include the population of the larger events.

Some of the larger secretory pole responses included in this analysis of the spikes are derived from signals that spread across the secretory pole and therefore might recruit more than one release site (such as the spike in Fig. 2; see also Kidd et al., 1999). We identified these spatially spreading Ca^{2+} spikes from the $\Delta F/F_0$ images, and these are indicated on the histogram (Fig. 5 *B*, *filled bars*). The signal

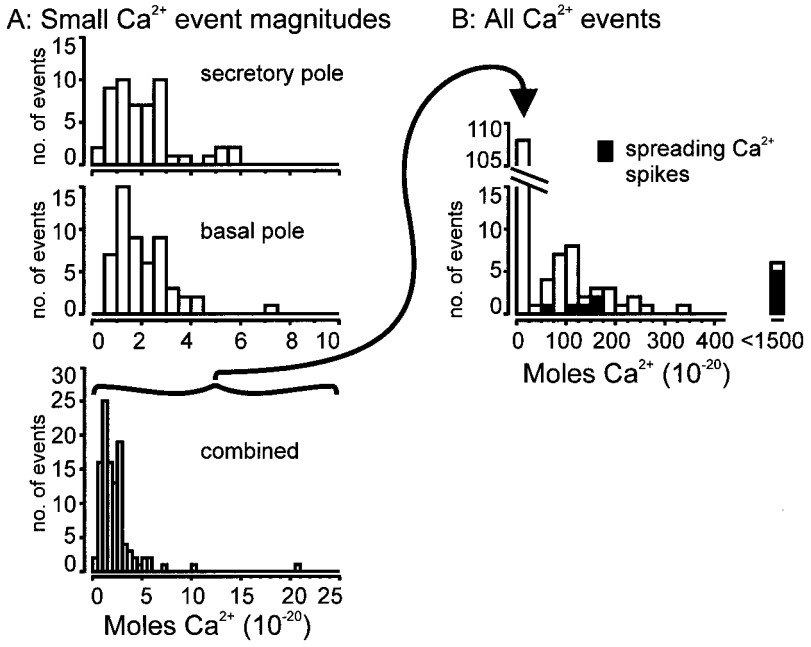

FIGURE 5 Histograms of the peak Ca^{2+} signal mass units of all Ca^{2+} events induced by $InsP_3$. *A* shows histograms of the small secretory pole ($n = 55$) and basal pole events ($n = 54$), respectively. No significant difference was found between these two distributions; therefore, the data are combined into a single histogram in the bottom part of the figure. This distribution of smaller events has a single mode of signal mass amplitudes. When these data are plotted together with the larger Ca^{2+} spikes, as shown in *B*, the smaller events appear as a single bin, corresponding to the expanded view (*arrow*) in *A*, *bottom*, and the larger events appear as a second mode of signal mass amplitudes clearly separated from the smaller events. The fraction of larger peak Ca^{2+} signal mass events contributed by "spreading" Ca^{2+} spikes, as identified from the $\Delta F/F_o$ images, are shown as filled bars. The smallest signal mass measured was equivalent to ~0.4 moles of Ca^{2+}.

mass units of these spikes were generally larger, which does affect the spread of the population of spikes but does not affect the clustering of spike amplitudes around the modal value. We conclude that the bimodal behavior, observed at constant $InsP_3$ concentrations, is the result of two different mechanisms of Ca^{2+} release.

Analysis of the peak Ca^{2+} signal mass therefore provides evidence that the smaller events and the spikes are derived from two separate populations of events. We characterized these events further by studying the time courses of the Ca^{2+} signal. The time course of the Ca^{2+} signal mass for smaller events in the basal pole and secretory pole are not significantly different, and are shown in Fig. 6, *A* and *B*. The Ca^{2+} spikes have been associated with the activation of $Cl_{(Ca)}$ currents, which are thought to be important for fluid secretion (Petersen, 1992). We therefore sought to determine whether the smaller Ca^{2+} events might also activate these currents and thus play a physiological role in secretion. The average $Cl_{(Ca)}$ current associated with the secretory pole Ca^{2+} event is shown in Fig. 6 *C*. No current was activated by the basal pole events (data not shown). Although there is a small current activated in synchrony with

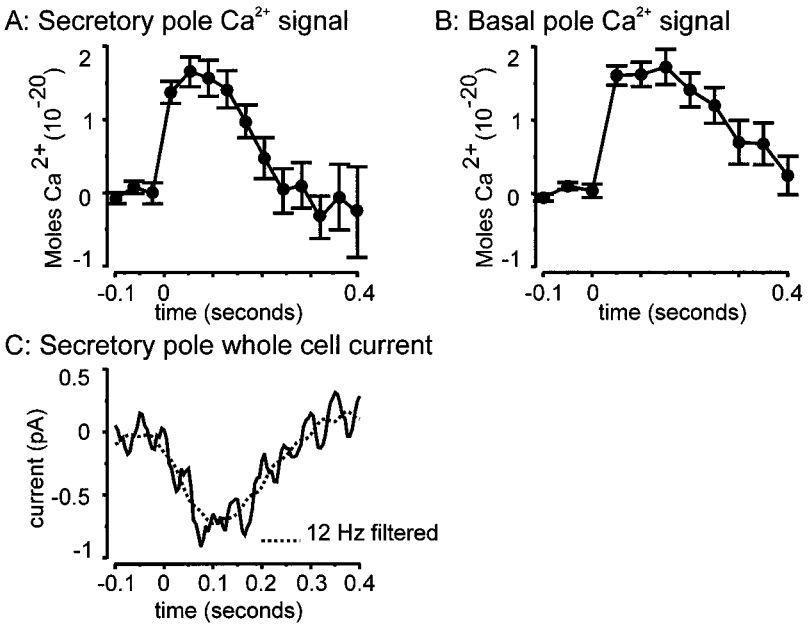

FIGURE 6 The average time courses of the Ca^{2+} signal during the secretory and basal pole small events, measured in signal mass units, are shown in *A* and *B* (data are shown as mean ± SEM). Before averaging, the small release events in the basal and secretory pole were aligned to the first significant Ca^{2+} increase above noise (indicated on graphs as time = 0 s). The Ca^{2+} signal mass rapidly rises to a peak and then decays more slowly back to baseline. The corresponding mean whole-cell current, simultaneously acquired with the secretory pole Ca^{2+} events, is shown in *C*. The basal pole events produced no significant whole-cell current.

the secretory pole Ca^{2+} events, the small size and low frequency of the Ca^{2+} event-induced $Cl_{(Ca)}$ current suggest they would play little role in fluid secretion. A similar analysis for the Ca^{2+} spikes (restricted to those that showed no evidence for a spread) demonstrated that the Ca^{2+} signal mass rose to a peak and then decayed relatively slowly compared to the $\Delta F/F_o$ images (Fig. 7). The average whole-cell current spike showed a large response. Interestingly, the peak current amplitude was ~70-fold greater than that induced by the small secretory pole Ca^{2+} events, which corresponds to the relative values for the peak Ca^{2+} signal mass units.

We can use our data to calculate the Ca^{2+} flux required to produce the Ca^{2+} signals observed. For each event we measured the time-to-peak and the peak Ca^{2+} signal mass amplitude, and then calculated the required Ca^{2+} current. This analysis gave a mean current of 0.058 pA and mean time-to-peak of 71.2 ms for the small Ca^{2+} event ($n = 106$) and a mean Ca^{2+} current of 0.399 pA and a mean time-to-peak of 1.19 s for the spikes ($n = 38$).

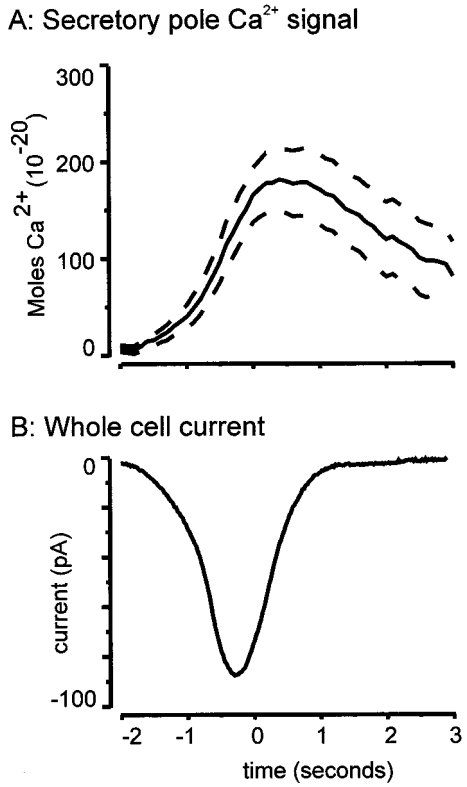

FIGURE 7 The average time course of the mean Ca^{2+} signal during the secretory pole spikes, measured in Ca^{2+} signal mass units, is shown in *A*. The solid line follows the mean values and the dotted lines represent the SEM range ($n = 39$). A relatively fast rise to a peak is followed by a decay back to baseline. The corresponding mean whole-cell current, simultaneously acquired with the secretory pole spikes, is shown in *B*.

DISCUSSION

Our data describe a bimodal pattern of spatially discrete Ca^{2+} signals in pancreatic acinar cells. This pattern, observed at constant $InsP_3$ concentrations, is not consistent with the smaller signals acting as building blocks for the larger spike. The population of larger Ca^{2+} spikes therefore appears to be a stereotypical unitary Ca^{2+} signal, which is not composed from the summation of the smaller events. The data indicate an additional, previously unrecorded, complexity to the Ca^{2+} signals in pancreatic acinar cells.

The range of the time course, the amplitude, and spatial spread of the Ca^{2+} events we observe are similar to those in *Xenopus* and HeLa cells. By these previous definitions, therefore, both the smaller Ca^{2+} signals and larger spikes seen in acinar cells are elementary events (Sun et al., 1998; Thomas et al., 1998). However, the pattern of Ca^{2+} signal mass distribution found in acinar cells is markedly different from the single population of elementary events described in *Xenopus* oocytes and HeLa cells. A direct comparison of our data with those of Sun et al. (1998), possible through the use of signal mass as a measurement of the Ca^{2+} signal, is informative. The data obtained in *Xenopus* show a decline in frequency of observing larger events, with only ~3% of their events above 100 Ca^{2+} signal mass units. This compares to the discrete population of ~25% of our total events that fall above this signal mass. Inasmuch as we observe that both the small and large Ca^{2+} signals have the same threshold for $InsP_3$ activation, we conclude that the larger spike is truly a unitary Ca^{2+} signal.

We do have evidence that the Ca^{2+} signal in some (25%) of the spikes does spread across the secretory pole. However, even if we exclude these events from the analysis we still observe the bimodal distribution of the Ca^{2+} signal mass (see Fig. 5). On this more macro scale, we have previously shown that the localized, oscillatory secretory pole signal induced by $InsP_3$ shows evidence for multiple sites of Ca^{2+} release (Thorn et al., 1996). In further experiments exogenous Ca^{2+} buffers were used to show that Ca^{2+} feedback is critical to the generation of these secretory pole responses (Kidd et al., 1999). In these experiments we demonstrated that Ca^{2+} release from up to three discrete sites in the secretory pole can be coordinated together to form the secretory pole Ca^{2+} signal. The Ca^{2+} spikes we describe in this paper originate from one of these discrete release sites, and the spreading events are where more than one site is recruited. It is only using the higher-resolution imaging techniques in this paper that we have now been able to resolve the smaller Ca^{2+} release events.

There are a number of possible mechanisms that might give rise to the bimodal behavior we observe. One possibility is that it is due to a differential distribution of $InsP_3$ receptors. The small events may arise from a site of a small cluster of $InsP_3$ receptors, the larger spikes from a larger cluster. In some cells, such as in Fig. 4, both smaller Ca^{2+}

events and the spikes appear to originate from the same region (although this is clearly limited by the resolution of our microscope). In other cells, such as shown in Fig. 1, they do not. If both events can arise from the same region of the cell, the bimodal behavior could be from recruitment of different numbers of $InsP_3$ receptors even within the site. Smaller Ca^{2+} release events, evoked at low concentrations of $InsP_3$ have been suggested to arise from a process of lateral Ca^{2+}-dependent inhibition (Adkins and Taylor, 1999). Whereas larger spikes may arise from a process of spreading excitability dependent on CICR at the $InsP_3$ receptor. However, from our work in acinar cells, both small events and larger Ca^{2+} spikes were seen at the same $InsP_3$ concentrations, with the same apparent threshold for $InsP_3$. We have to conclude, therefore, that the mechanisms of production of the two Ca^{2+} signals are not differentially dependent on $InsP_3$ concentration. Sequential recruitment of Ca^{2+} release has been seen in HeLa cells where miniature waves were observed across a release site (Bootman et al., 1997a). These observations are consistent with the continuum of events sizes observed in HeLa cells, but contrast to work in *Xenopus* oocytes that describes the continuum of elementary events as coming from a point source (Sun et al., 1998).

Another possible explanation for bimodal activity is that different $InsP_3$ receptor isoforms underlie the two events. It is now well-documented that $InsP_3$ receptor isoforms have a range of different characteristics. Pancreatic acinar cells predominantly express the type 2 and type 3 $InsP_3$ receptor isoforms (De Smedt et al., 1997; Wojcikiewicz, 1995). The type 2 receptor is exclusively located in the secretory pole (Lee et al., 1997; Yule et al., 1997) and therefore this is a likely candidate receptor to underlie the larger Ca^{2+} spikes. In support of this, expression of type 2 receptors has been shown to be specifically important in the generation of oscillations (Miyakawa et al., 1999) and the type 2 receptor shows a higher affinity for $InsP_3$ (Newton et al., 1994; Parys et al., 1995). Recently, the type 3 $InsP_3$ receptor has been proposed as a candidate for the initiation of the Ca^{2+} signal in acinar cells, largely based on the lack of Ca^{2+}-dependent inactivation seen in receptors purified and recorded from within bilayers (Hagar et al., 1998). However, this non-inactivating behavior is not seen permeabilized in 16HBE14o- bronchial mucosal cells that predominantly express the type 3 receptor (Missiaen et al., 1998). Furthermore, the type 2 $InsP_3$ receptor, purified and recorded in a lipid bilayer, has also been shown to lack Ca^{2+}-dependent inactivation (Ramos-Franco et al., 1998). The similar apparent threshold and dependence on $InsP_3$ of the small events and larger spikes argues that simple receptor affinity for $InsP_3$ is not the basis of the two Ca^{2+} signals. Clearly further work, concentrating on recording from $InsP_3$ receptors intact in their native environment, will be required to resolve these issues (Taylor, 1998). It remains an attractive proposal that the bimodal behavior we observe is the result of different Ca^{2+} release mechanisms from two different $InsP_3$ receptor isoforms.

We thank Professor Lawrence Lifshitz for his help and advice with the computer simulations. The work was started as a collaboration funded by the Human Frontiers in Science Programme between P.T. and Professor Fred Fay, and we dedicate this paper to the memory of Fred.

This work was supported by The Wellcome Trust, the Medical Research Council (project grant to P.T. and Dr. T. R. Cheek), and The Royal Society (project grant to P.T.), the National Science Foundation (Grants DBI-9200027 and DBI-9724611), and the National Institutes of Health (R01 grant to Walter Carrington 5RR09799). J.F.K. is in receipt of a Biotechnological and Biological Sciences Research Council Studentship.

REFERENCES

Adkins, C. E., and C. W. Taylor 1999. Lateral inhibition of inositol 1,4,5-trisphosphate receptors by cytosolic Ca^{2+}. *Curr. Biol.* 9:1115–1118.

Berridge, M. J. 1997. Elementary and global aspects of calcium signalling. *J. Physiol. (Lond.).* 499(Pt. 2):290–306.

Bootman, M. D., M. J. Berridge, and P. Lipp. 1997b. Cooking with calcium: the recipes for composing global signals from elementary events. *Cell.* 91:367–373.

Bootman, M., E. Niggli, M. Berridge, and P. Lipp. 1997a. Imaging the hierarchical Ca^{2+} signalling system in HeLa cells. *J. Physiol. (Lond.).* 499(Pt. 2):307–314.

Callamaras, N., J. S. Marchant, X. P. Sun, and I. Parker. 1998. Activation and co-ordination of InsP3-mediated elementary Ca^{2+} events during global Ca^{2+} signals in *Xenopus* oocytes. *J. Physiol. (Lond.).* 509(Pt. 1):81–91.

Deisseroth, K., E. K. Heist, and R. W. Tsien. 1998. Translocation of calmodulin to the nucleus supports CREB phosphorylation in hippocampal neurons. *Nature.* 392:198–202.

De Koninck, P., and H. Schulman. 1998. Sensitivity of CaM kinase II to the frequency of Ca^{2+} oscillations. *Science.* 279:227–230.

De Smedt, H., L. Missiaen, J. B. Parys, R. H. Henning, I. Sienaert, S. Vanlingen, A. Gijsens, B. Himpens, and R. Casteels. 1997. Isoform diversity of the inositol trisphosphate receptor in cell types of mouse origin. *Biochem. J.* 322(Pt. 2):575–583.

Dolmetsch, R. E., K. Xu, and R. S. Lewis. 1998. Calcium oscillations increase the efficiency and specificity of gene expression [see comments]. *Nature.* 392:933–936.

Hagar, R. E., A. D. Burgstahler, M. H. Nathanson, and B. E. Ehrlich. 1998. Type III InsP3 receptor channel stays open in the presence of increased calcium. *Nature.* 396:81–84.

Hamill, O. P., A. Marty, E. Neher, B. Sakmann, and F. J. Sigworth. 1981. Improved patch-clamp techniques for high-resolution current recording from cells and cell-free membrane patches. *Pflugers Arch.* 391:85–100.

Ito, K., Y. Miyashita, and H. Kasai. 1997. Micromolar and submicromolar Ca^{2+} spikes regulating distinct cellular functions in pancreatic acinar cells. *EMBO J.* 16:242–251.

Ito, K., Y. Miyashita, and H. Kasai. 1999. Kinetic control of multiple forms of $Ca(^{2+})$ spikes by inositol trisphosphate in pancreatic acinar cells. *J. Cell Biol.* 146:405–413.

Kasai, H., Y. X. Li, and Y. Miyashita. 1993. Subcellular distribution of Ca^{2+} release channels underlying Ca^{2+} waves and oscillations in exocrine pancreas. *Cell.* 74:669–677.

Kidd, J. F., K. E. Fogarty, R. Tuft, and P. Thorn. 1999. The role of Ca^{2+} feedback in shaping InsP3-evoked Ca^{2+} signals in mouse pancreatic acinar cells. *J. Physiol.* 520.1:187–201.

Lee, M. G., X. Xu, W. Zeng, J. Diaz, R. J. Wojcikiewicz, T. H. Kuo, F. Wuytack, L. Racymaekers, and S. Muallem. 1997. Polarized expression of Ca^{2+} channels in pancreatic and salivary gland cells. Correlation with

initiation and propagation of [Ca^{2+}]i waves. *J. Biol. Chem.* 272: 15765–15770.

Mak, D. O., and J. K. Foskett. 1997. Single-channel kinetics, inactivation, and spatial distribution of inositol trisphosphate (IP3) receptors in *Xenopus* oocyte nucleus. *J. Gen. Physiol.* 109:571–587.

Miyakawa, T., A. Maeda, T. Yamazawa, K. Hirose, T. Kurosaki, and M. Iino. 1999. Encoding of Ca^{2+} signals by differential expression of IP3 receptor subtypes. *EMBO J.* 18:1303–1308.

Missiaen, L., J. B. Parys, I. Sienaert, K. Maes, K. Kunzelmann, M. Takahashi, K. Tanzawa, and H. De Smedt. 1998. Functional properties of the type-3 InsP3 receptor in 16HBE14o- bronchial mucosal cells. *J. Biol. Chem.* 273:8983–8986.

Nelson, M. T., H. Cheng, M. Rubort, L. F. Santana, A. D. Bonev, H. J. Knot, and W. J. Lederer. 1995. Relaxation of arterial smooth muscle by calcium sparks. *Science.* 270:633–637.

Newton, C. L., G. A. Mignery, and T. C. Südhof. 1994. Co-expression in vertebrate tissues and cell lines of multiple inositol 1,4,5-trisphosphate (InsP3) receptors with distinct affinities for InsP3. *J. Biol. Chem.* 269: 28613–28619.

Parys, J. B., H. de Smedt, L. Missiaen, M. D. Bootman, I. Sienaert, and R. Casteels. 1995. Rat basophilic leukemia cells as model system for inositol 1,4,5-trisphosphate receptor IV, a receptor of the type II family: functional comparison and immunological detection. *Cell Calcium.* 17: 239–249.

Petersen, O. H. 1992. Stimulus-secretion coupling: cytoplasmic calcium signals and the control of ion channels in exocrine acinar cells. *J. Physiol. (Lond.).* 448:1–51.

Ramos-Franco, J., M. Fill, and G. A. Mignery. 1998. Isoform-specific function of single inositol 1,4,5-trisphosphate receptor channels. *Biophys. J.* 75:834–839.

Rizzuto, R., P. Pinton, W. Carrington, F. S. Fay, K. E. Fogarty, L. M. Lifshitz, R. A. Tuft, and T. Pozzan. 1998. Close contacts with the endoplasmic reticulum as determinants of mitochondrial Ca^{2+} responses. *Science.* 280:1763–1766.

Sun, X. P., N. Callamaras, J. S. Marchant, and I. Parker. 1998. A continuum of InsP3-mediated elementary Ca^{2+} signalling events in *Xenopus* oocytes. *J. Physiol. (Lond.).* 509(Pt.1):67–80.

Taylor, C. W. 1998. Inositol trisphosphate receptors: Ca^{2+}-modulated intracellular Ca^{2+} channels. *Biochim. Biophys. Acta.* 1436:19–33.

Thomas, D., P. Lipp, M. J. Berridge, and M. D. Bootman. 1998. Hormone-evoked elementary Ca^{2+} signals are not stereotypic, but reflect activation of different size channel clusters and variable recruitment of channels within a cluster. *J. Biol. Chem.* 273:27130–27136.

Thorn, P., O. Gerasimenko, and O. H. Petersen. 1994. Cyclic ADP-ribose regulation of ryanodine receptors involved in agonist evoked cytosolic Ca^{2+} oscillations in pancreatic acinar cells. *EMBO J.* 13:2038–2043.

Thorn, P., A. M. Lawrie, P. M. Smith, D. V. Gallacher, and O. H. Petersen. 1993. Local and global cytosolic Ca^{2+} oscillations in exocrine cells evoked by agonists and inositol trisphosphate. *Cell.* 74:661–668.

Thorn, P., R. Moreton, and M. Berridge. 1996. Multiple, coordinated Ca^{2+}-release events underlie the inositol trisphosphate-induced local Ca^{2+} spikes in mouse pancreatic acinar cells. *EMBO J.* 15:999–1003.

Thorn, P., and O. H. Petersen. 1992. Activation of nonselective cation channels by physiological cholecystokinin concentrations in mouse pancreatic acinar cells. *J. Gen. Physiol.* 100:11–25.

Wakui, M., and O. H. Petersen. 1990. Cytoplasmic Ca^{2+} oscillations evoked by acetylcholine or intracellular infusion of inositol trisphosphate or Ca^{2+} can be inhibited by internal Ca^{2+}. *FEBS Lett.* 263: 206–208.

Wojcikiewicz, R. J. 1995. Type I, II, and III inositol 1,4,5-trisphosphate receptors are unequally susceptible to down-regulation and are expressed in markedly different proportions in different cell types. *J. Biol. Chem.* 270:11678–11683.

Yao, Y., J. Choi, and I. Parker. 1995. Quantal puffs of intracellular Ca^{2+} evoked by inositol trisphosphate in *Xenopus* oocytes. *J. Physiol. (Lond.).* 482(Pt. 3):533–553.

Yule, D. I., S. A. Ernst, H. Ohnishi, and R. J. Wojcikiewicz. 1997. Evidence that zymogen granules are not a physiologically relevant calcium pool. Defining the distribution of inositol. 1,4,5-trisphosphate receptors in pancreatic acinar cells. *J. Biol. Chem.* 272:9093–9098.

Zou, H., L. M. Lifshitz, R. A. Tuft, K. E. Fogarty, and J. J. Singer. 1999. Imaging Ca^{2+} entering the cytoplasm through a single opening of a plasma membrane cation channel. *J. Gen. Physiol.* 114:575–588.